Density-Functional Study on the Structures, Stabilities, and Dissociation Pathways of $Sc^{3+}(DMSO)_n$ Complexes ($n = 1-6$)

Chuanyun Xiao,[†] Frank Hagelberg,*[,†] and Ahmed M. El-Nahas[‡]

Computational Center for Molecular Structure and Interactions, Department of Physics, Atmospheric Sciences and General Science, Jackson State University, Jackson, Mississippi 39217, and Chemistry Department, Faculty of Science, El-Menoufia University, Shebin El-Kom, Egypt

Received: November 26, 2003; In Final Form: February 9, 2004

A comprehensive theoretical study is performed on $Sc^{3+}(DMSO)_n$ complexes up to $n = 6$ at the B3LYP/6-311+G(d, p) level to understand their structures and stabilities with respect to various dissociation channels, including the evaporation of neutral DMSO, the dissociative electron and proton transfer, the cleavage of a methyl radical (CH_3) and methane (CH_4) as well as their combined loss ($2CH_3$, $2CH_4$, and $CH_3 + CH_4$). The most stable structures of $Sc^{3+}(DMSO)_n$ correspond to highly symmetric and quasi-spherical configurations. The calculated dissociation energies indicate that the $Sc^{3+}(DMSO)_n$ species are thermodynamically stable with respect to all considered dissociation processes without charge separation for any size and to the charge-separating processes (dissociative electron transfer and loss of CH_3^+) for $n \geq 4$ but are thermodynamically unstable with respect to these charge-separating processes for $n = 1-3$. The transition states for the charge-separating processes of $Sc^{3+}(DMSO)_n$ with $n = 1-3$ are determined, and the calculated energy barriers are found to be high enough to stabilize the respective complex. Therefore, these small species are kinetically metastable with long lifetimes and should be observable. The minimum number (n_{min}) of DMSO ligands required to stabilize the Sc^{3+} ion against dissociative electron or proton transfer emerges from our calculations as $n_{min} = 1$, and the critical size (n_{crit}), above which the evaporation of a neutral ligand becomes more favorable than the dissociative electron or proton transfer, is estimated to be $n_{crit} = 5-6$.

I. Introduction

The study of ion solvation in liquids has been at the heart of physical chemistry since its inception a century ago.[1] Recently, attention has moved to ion solvation in finite systems, where the elementary processes can be followed stepwise by mass-spectrometric methods[2,3] and a close connection to high-level theoretical modeling is possible. These microscopic studies in finite systems are of great benefit for the thorough understanding of chemical processes in solution.

Solvation of metal ions is particularly intriguing in view of the critical importance of coordination effects involving organic ligands (self-solvation) in many biological molecules.[4,5] Although gas-phase metal−ligand complexes have been studied for several decades, most work was limited to singly charged species because solvated multiply charged metal ions were not accessible until the 1990s. The difficulty in generating multiply charged metal−ligand complexes results from the generally huge difference between the second ionization energy (IE_2) of a metal and the first IE (IE_1) of a ligand. The IE_1 of most common organic ligands lies in the range of 8−12 eV,[6] while the IE_2's of almost all metal atoms (except alkaline earths) are above 12 eV. Hence, electron transfer from a neutral ligand (L) to a bare metal (M) dication is usually energetically favorable and occurs spontaneously upon contact followed by dissociation driven by Coulombic repulsion,[7] namely, $M^{2+}L_n \rightarrow M^+L_{n-1} + L^+$. This tendency is even more pronounced for metal trications since the third IE (IE_3) of all metals lies above 19 eV, and charge reduction takes place upon contact with any ligand. This hinders sequential ligation of multiply charged metal ions in the manner that is standard for singly charged ones—by passing through the vapor of a desired ligand species. Even the metal dications with IE_2 below the ligand IE_1 that do not undergo electron transfer can often not be ligated by sequential addition, due to the existence of other competitive dissociation processes, including proton transfer[7−9] and a variety of intraligand cleavage processes, with or without charge reduction.

A decade ago, ligated multiply charged metal ions were successfully produced by the electrospray ionization (ESI) technique.[10] This technique circumvents the small size range, where the simultaneous dissociative electron or proton transfer would occur, by transferring the solvated ions already existing in liquid solution directly into the gas phase. More recently, two other alternative techniques, the so-called "pick-up"[11] and "charge-stripping"[12] methods, were developed, which generate the multiply charged metal−ligand complexes by laser or electron-impact ionization of the presolvated metal neutrals or monocations.

These methods have generated gas-phase complexes of metal dications with a variety of ligands, including both protic (water, alcohols) and aprotic (ethers, acetone, acetonitrile, ketones, dimethyl sulfoxide (DMSO), benzene, and pyridine) solvents.[9,13−19] The production of these species becomes more challenging with the increase of the IE_2 of the metal atoms.

In comparison, microsolvated metal trications have been reported only for one protic ligand (diacetone alcohol)[20] and four aprotic ones (DMSO, dimethyl formamide, acetone, and acetonitrile),[21−24] and the metal atoms belong exclusively to

* Corresponding author. E-mail: frank.d.hagelberg@ccaix.jsums.edu.
† Jackson State University.
‡ El-Menoufia University.

10.1021/jp031280i CCC: $27.50
Published on Web 06/02/2004

group 3 in the periodic table, including yttrium and the lanthanides, which have the lowest IE_3 of all metals.

Very recently, Shvartsburg[25] reported the formation of DMSO complexes for a number of triply charged ions of metals including scandium and those not belonging to group 3, both main group (Al, Ga, In, Bi) and transition metals (V, Cr, Fe), using the ESI technique. This is the first observation of microsolvated trications for metals beyond group 3.

Two parameters are introduced to characterize the stability of multiply charged complexes against charge reduction in the gas phase:[19,20,24] the minimum and the critical size. While a bare metal dication or trication may spontaneously transfer charge (electron or proton) to a neutral ligand in the gas phase as described above, these species are stable in bulk solution. Therefore, there must be a minimum size (n_{min}) of ligands at which the complex is stable with respect to a spontaneous electron or proton transfer. In addition, macroscopic droplets dissociate only by evaporating neutral ligands. Thus, there exists a critical size (n_{crit}) above which the loss of a neutral ligand becomes more favorable than dissociative electron or proton transfer. For complexes with $n_{min} < n \leq n_{crit}$, the loss of neutral ligands and the dissociative electron or proton transfer compete. For various cleavage processes, individual critical sizes can be defined in an analogous way.[19]

On the theoretical side, the existence of a variety of metal dications solvated by water, ammonia, formaldehyde, acetone, and DMSO has been investigated by ab initio quantum chemical methods.[26−28] These studies predicted that, although most of the studied monosolvated metal dications are thermodynamically unstable in the gas phase because of spontaneous charge transfer, these systems are kinetically metastable and thus experimentally detectable due to the existence of an energy barrier formed by the avoided crossing of the attractive $M^{2+}-L$ potential with the repulsive Coulombic potential of the charge-separation products $M^+ + L^+$,[12,26] and the calculated results were supported by recent experimental findings[9,29,30] using charge-stripping and electrospray ionization techniques. However, these theoretical studies are limited to complexes with one or two ligands and to the electron-transfer process only. Few calculations have dealt with competitive proton transfer[8,31] and other intraligand cleavage processes,[32,33] and no theoretical exploration of n_{crit} has been reported.

Stimulated by the experimental as well as theoretical progress in the field of multiligated metal cations, we have initiated a comprehensive study of the structures, stability, and various dissociation channels of multiply charged metal−ligand complexes. In the recent experimental work of Shvartsburg,[25] rich dissociation chemistry of $M^{3+}(DMSO)_n$ was observed. For the Sc^{3+} complexes, it was found that they dissociate neither by electron transfer nor by proton transfer as was observed for $M^{2+}(H_2O)_n$.[9] Rather, the $Sc^{3+}(DMSO)_n$ species dissociate by various intraligand cleavage processes, most prominently the loss of a methyl radical or a methyl cation (CH_3 or CH_3^+), the loss of methane (CH_4), and a combined loss of CH_3 and CH_4. Motivated by these experimental findings, we chose the $Sc^{3+}(DMSO)_n$ species ($n = 1-6$) in this work and studied their structures, stabilities, and energetics in the following selected dissociation processes: the loss of DMSO (neutral evaporation), the loss of $DMSO^+$ (electron transfer), the loss of H^+DMSO (proton transfer), the loss of CH_3 and CH_4 as well as their combinations ($2CH_3$, $2CH_4$, and $CH_3 + CH_4$) and cations (CH_3^+ and CH_4^+). The following problems will be addressed:

(1) What are the equilibrium structures of $Sc^{3+}(DMSO)_n$?

(2) What are the structures of various dissociation products, and what are the related dissociation energies?

(3) Are the $Sc^{3+}(DMSO)_n$ complexes stable with respect to these dissociation processes? If not, what are the structures of the transition states for these dissociation processes and are the respective energy barriers sufficiently high to prevent the metal−ligand complexes from spontaneous dissociation?

(4) What are the minimum and critical sizes for the $Sc^{3+}(DMSO)_n$ complexes?

The paper is arranged as follows: the computational details are described in Section II, the results are presented and discussed in Section III, and a summary is given in Section IV.

II. Computational Details

The geometries of $Sc^{3+}(DMSO)_n$, different dissociation products, and related transition states, as well as DMSO, $DMSO^+$, and $Sc^{2+}(DMSO)_n$ were fully optimized without symmetry constraints using the B3LYP hybrid density-functional method in conjunction with the 6-311+G(d, p) basis set implemented in the Gaussian 98 program.[34] The B3LYP density functional consists of a combination of Becke's three-parameter exchange functional[35] (B3) with Lee, Yang, and Parr's (LYP) correlation functional.[36] This method with similar or smaller basis sets has been applied successfully to study the structures and dissociation processes for the complexes of alkaline and transition metal dications ligated with H_2O, NH_3, acetone, and DMSO.[8,26−28,32,33]

For each species of $Sc^{3+}(DMSO)_n$, several starting geometries were selected for optimization in order to determine the energetically lowest structure. For the monoligated species, optimizations at the B3LYP/6-31+G(d) and MP2/6-311+G(d, p) levels were performed, and the optimized geometries were found to be very close to those obtained at the B3LYP/6-311+G(d, p) level. The search for the transition states (TS) associated with the charge-separating processes (electron transfer and loss of CH_3^+) proved to be challenging; to identify these states, we have used several techniques, including the synchronous transit-guided quasi-Newton (QST3) and the eigenvalue-following (EF) optimization procedures.

All structures reported here have been verified to be local minima (no imaginary frequencies) or transition states (one imaginary frequency) on their respective potential energy surfaces by frequency analysis at the B3LYP/6-311+G(d, p) level, with the exception of $Sc^{3+}(DMSO)_5$ and $Sc^{3+}(DMSO)_6$ whose stability was confirmed only at the B3LYP/3-21G* level, as necessitated by the considerable sizes of these systems.

The zero-point energy (ZPE) and basis set superposition error (BSSE) corrections were estimated for selected species. The BSSE correction was calculated by the counterpoise method of Boys and Bernardi,[37] with the geometry of the ligands fixed to that in the optimized complex. For the representative Sc^{3+}-DMSO species, the ZPE and BSSE corrections were found to amount only to 0.14% and 0.43%, respectively, of the metal−ligand binding energy. Therefore, the reported energies are neither ZPE nor BSSE corrected.

The atomic charges were calculated with the natural bond orbital (NBO) program[38] implemented in the Gaussian 98 package using the B3LYP/6-311+G(d, p) densities.

III. Results and Discussion

In the following, we will first describe the structures for $Sc^{3+}(DMSO)_n$, various dissociation products, and transition states, and then analyze the energetic properties of these dissociation processes.

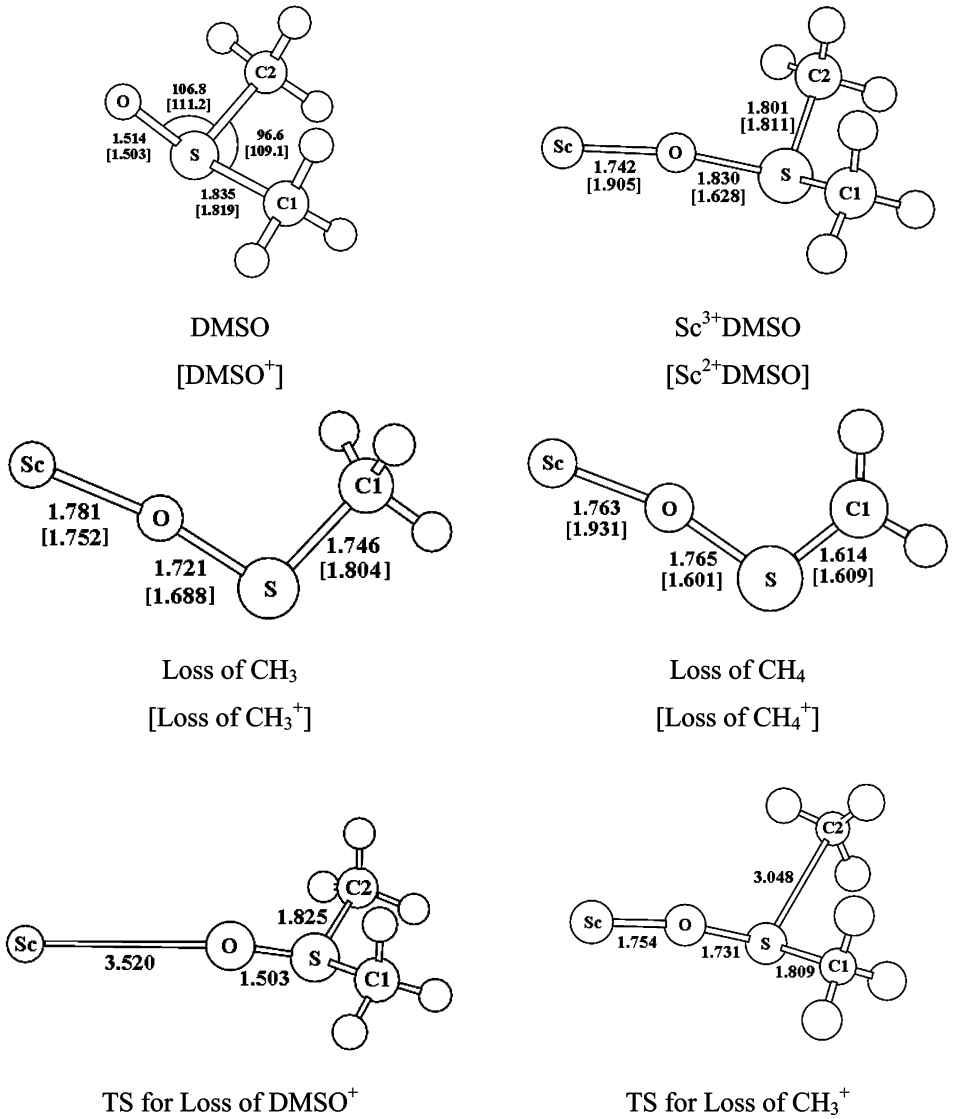

Figure 1. Structures (in angstroms and degrees) for DMSO, Sc^{3+}DMSO, and various dissociated products as well as related transition states (TS), obtained at the B3LYP/6-311+G(d, p) level. Unlabeled open circles stand for hydrogen atoms.

III.A. Structures. The optimized geometries with the main structural parameters for $Sc^{3+}(DMSO)_n$, various dissociation products, and transition states, as well as DMSO, $DMSO^+$, and $Sc^{2+}(DMSO)_n$ are shown in Figures 1−4. The Sc atom is attached to the O atoms in all complexes. More complete geometrical data and natural charges are available in the Supporting Information.

The O−S and S−C bond lengths in neutral DMSO are 1.514 and 1.835 Å and the O−S−C and C−S−C bond angles are 106.8° and 96.6°, respectively. In $DMSO^+$, the ionization leads to a slight decrease of the two bond lengths and an increase of the two bond angles.

For a single DMSO ligand, the addition of a Sc^{3+} trication leads to considerable elongation of the O−S bond, a slight decrease of the S−C bond, and an increase of the O−S−C and C−S−C angles as compared with neutral DMSO. The Sc−O and O−S bonds include an angle of 168.2°.

Two bent isomers were identified for $Sc^{3+}(DMSO)_2$ which differ in the orientation of their second DMSO by 180°. The O−Sc−O bending angles are 122.3° and 124.8°, respectively. Other bond lengths and angles of these two conformations are also quite similar. The energies of these two isomers are nearly the same, with a slight energy margin of 1.5 kcal/mol, indicating that the detailed orientations of the DMSOs in a given configuration have negligible impact on the energy. Here we describe the configuration (and symmetry, see below) of a complex by idealizing the ligands as simple lines and ignoring their structural details.

We have calculated the dissociation energies (E_d) for the following two processes: (1) $Sc^{3+}(DMSO)_2 \rightarrow Sc^{3+} + 2DMSO$ and (2) $Sc^{3+}(DMSO)_2 \rightarrow Sc^{3+} + (DMSO)_2$ [fixed at the geometry adopted in optimized $Sc^{3+}(DMSO)_2$] and found that E_d1, E_d2 are 504.4 and 533.0 kcal/mol, respectively. E_d1 includes the Sc^{3+}−ligand and the ligand−ligand interactions, and E_d2 roughly represents the Sc^{3+}−ligand interaction. The difference between E_d1 and E_d2 thus reflects the interaction between the two DMSO ligands, which is only 28.6 kcal/mol. Therefore, the stabilization of the $Sc^{3+}(DMSO)_2$ complex is predominantly attributed to the metal−ligand interaction while the interligand interaction is weak. Such weak interaction between ligands is also observed in larger $Sc^{3+}(DMSO)_n$ species. Natural population analysis indicates that the ligands in $Sc^{3+}(DMSO)_n$ all carry a net positive charge (+0.65 for $n = 1$; +0.39 for $n = 2$; +0.28 for $n = 3$; and +0.25 for $n = 4$). As a result of the Coulombic repulsion, the DMSO ligands tend to avoid each other and spread as far as possible in space. Therefore, the most stable structures

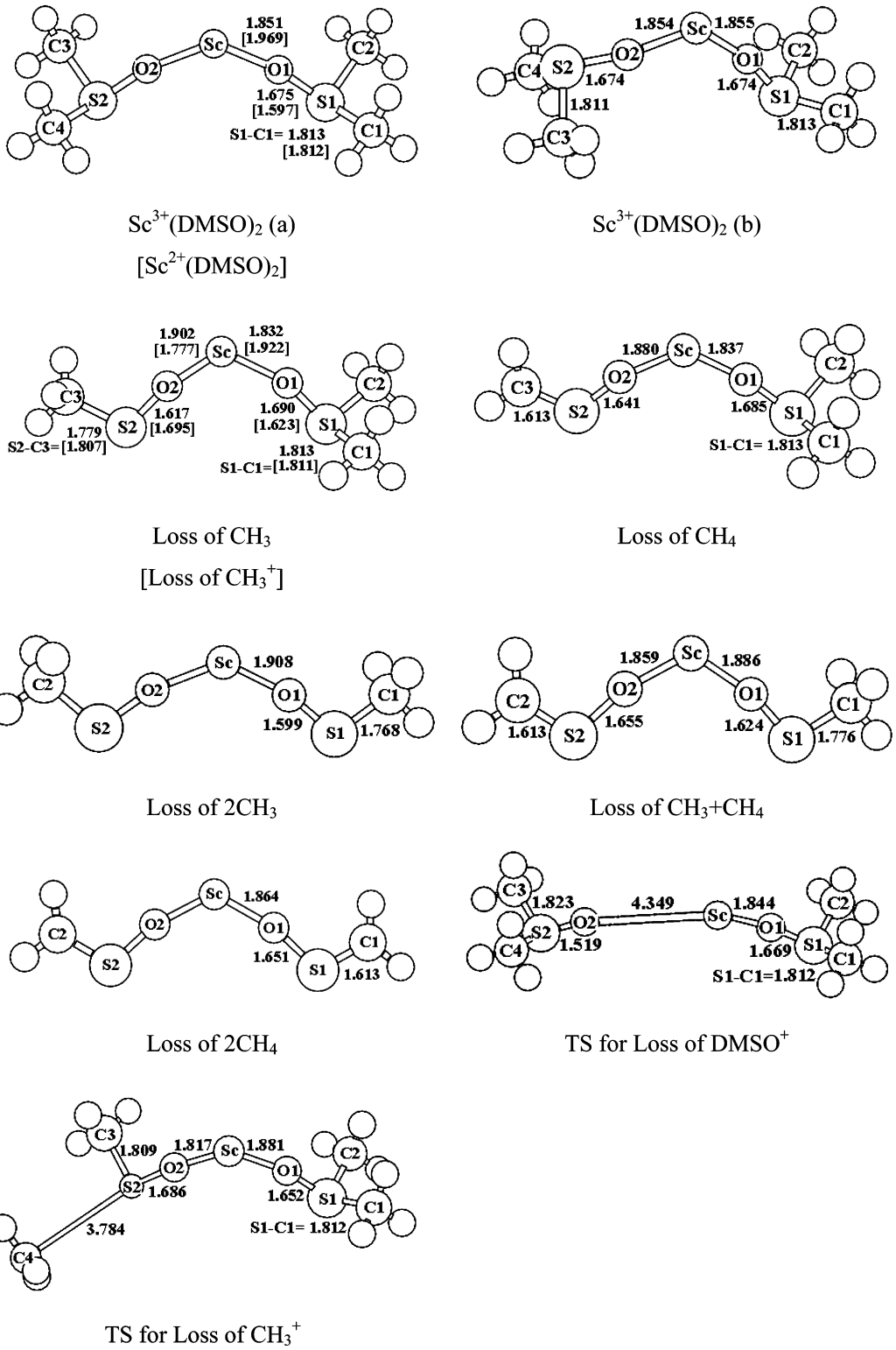

$Sc^{3+}(DMSO)_2$ (a)
$[Sc^{2+}(DMSO)_2]$

$Sc^{3+}(DMSO)_2$ (b)

Loss of CH_3
$[Loss\ of\ CH_3^+]$

Loss of CH_4

Loss of $2CH_3$

Loss of CH_3+CH_4

Loss of $2CH_4$

TS for Loss of $DMSO^+$

TS for Loss of CH_3^+

Figure 2. Structures (in angstroms) for $Sc^{3+}(DMSO)_2$ and various dissociated products as well as related transition states (TS), obtained at the B3LYP/6-311+G(d, p) level. Unlabeled open circles stand for hydrogen atoms.

for larger $Sc^{3+}(DMSO)_n$ complexes all correspond to highly symmetric and quasi-spherical ones, namely, an equilateral triangle for $Sc^{3+}(DMSO)_3$, a tetrahedron for $Sc^{3+}(DMSO)_4$, a trigonal bipyramid for $Sc^{3+}(DMSO)_5$, and an octahedron for $Sc^{3+}(DMSO)_6$.

In our calculations of $Sc^{3+}(DMSO)_3$ and $Sc^{3+}(DMSO)_4$, many initial structures were considered in the geometry optimization. For $Sc^{3+}(DMSO)_3$, the three DMSO ligands were attached to the central Sc^{3+} ion in triangular configurations with various in-plane and off-plane orientations, and we found that these configurations are different in energy within 1 kcal/mol. For $Sc^{3+}(DMSO)_4$, the four DMSO ligands were coordinated to the central Sc^{3+} ion in planar square or tetrahedral configurations with various orientations. Similar to the observation in Sc^{3+}-$(DMSO)_3$, the tetrahedral configurations with various ligand orientations differ in energy from each other by negligible amounts (within 0.6 kcal/mol), while the planar structures were found to be transition states and to relax to the tetrahedral ones

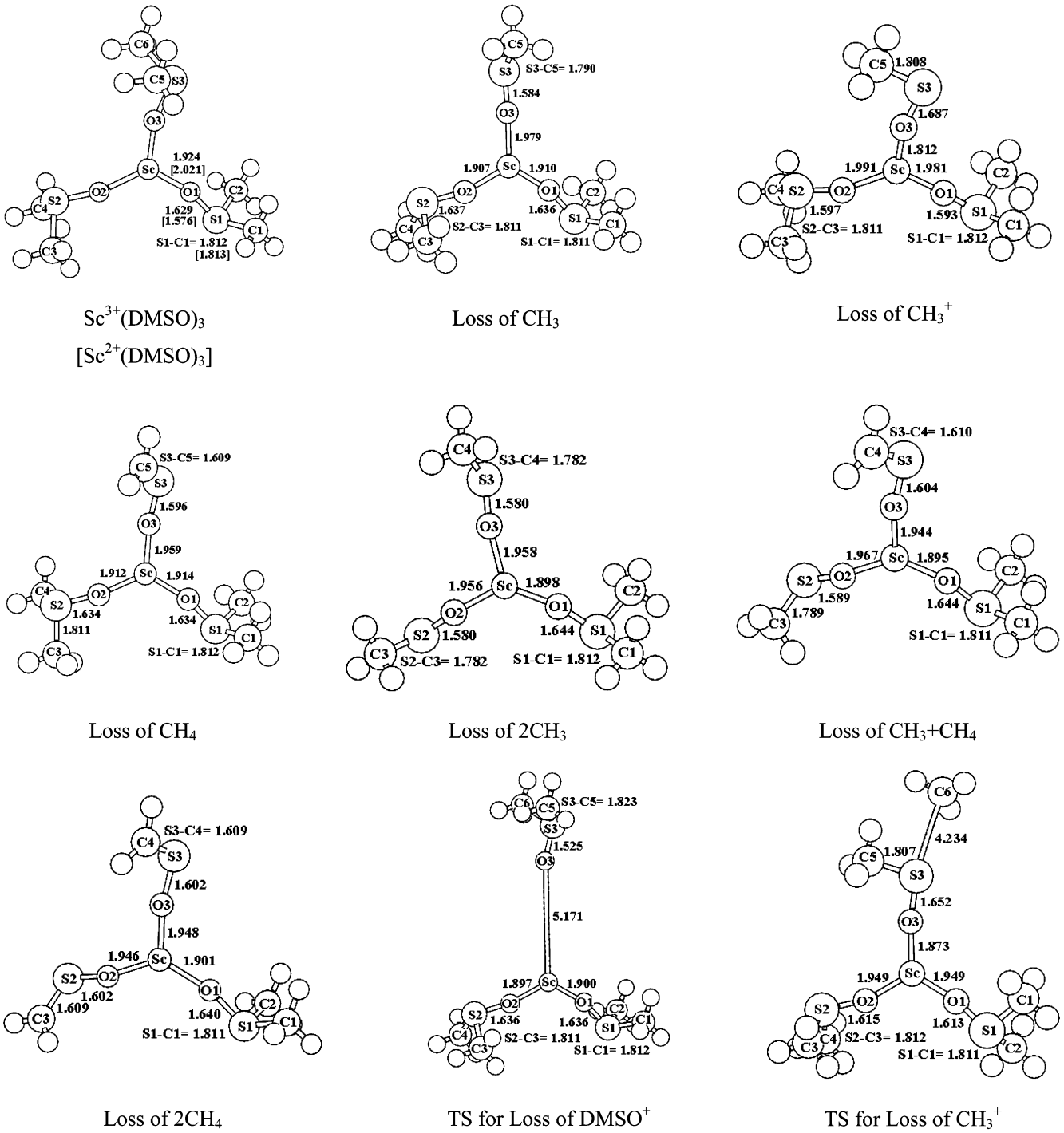

Figure 3. Structures (in angstroms) for $Sc^{3+}(DMSO)_3$ and various dissociated products as well as related transition states (TS), obtained at the B3LYP/6-311+G(d, p) level. Unlabeled open circles stand for hydrogen atoms.

with an energy gain of 23.0 kcal/mol. As seen in Figures 2−4, the structure of $Sc^{3+}(DMSO)_3$ can be understood to arise from attaching a third DMSO to $Sc^{3+}(DMSO)_2$ (b) while Sc^{3+}-$(DMSO)_4$ is composed of two perpendicular $(DMSO)_2$ pairs, each of them arranged as in $Sc^{3+}(DMSO)_2$ (b) and both coordinated by a central Sc^{3+} unit.

In analogy to $Sc^{3+}(DMSO)_4$, both planar pentagonal and trigonal bipyramidal structures were taken into account for Sc^{3+}-$(DMSO)_5$. The planar conformation is higher in energy than the trigonal bipyramid by 48.0 kcal/mol. In view of the results for $Sc^{3+}(DMSO)_4$ and $Sc^{3+}(DMSO)_5$, we no longer considered the planar structure and assumed an octahedral configuration for $Sc^{3+}(DMSO)_6$. For both $Sc^{3+}(DMSO)_5$ and $Sc^{3+}(DMSO)_6$, the stability was confirmed by frequency calculation only at the lower B3LYP/3-21G* level.

As seen from Figures 1−4, with increasing size of Sc^{3+}-$(DMSO)_n$ up to $n = 6$, the Sc−O bond length is elongated from 1.742 to 2.122 Å, the O−S bond length is shortened from 1.830 to 1.571 Å, while the S−C distance remains nearly unchanged. As for the bond angles, the Sc−O−S angle decreases from 168.2° to 135.9°, and the O−S−C and C−S−C angles are almost unaltered. From population analysis, we can also find that the natural charge on the Sc ion decreases gradually from 2.34 to 1.90 *e*, and the charges on the O, S, C, and H atoms are nearly unchanged with the increasing size.

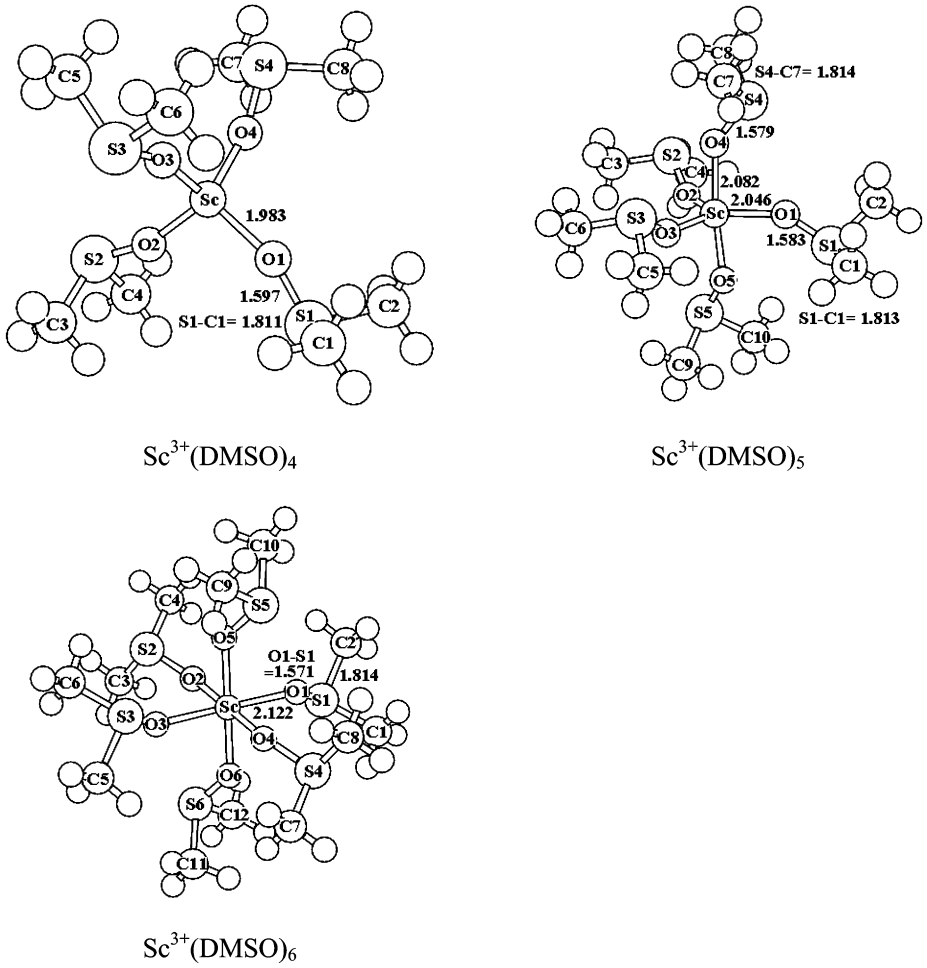

$Sc^{3+}(DMSO)_4$ $Sc^{3+}(DMSO)_5$

$Sc^{3+}(DMSO)_6$

Figure 4. Structures (in angstroms) for $Sc^{3+}(DMSO)_n$ ($n = 4-6$), obtained at the B3LYP/6-311+G(d, p) level. Unlabeled open circles stand for hydrogen atoms.

On the basis of the above results for $Sc^{3+}(DMSO)_n$, we further studied the dissociation of these complexes in the following processes:

(a) Loss of charged DMSO (electron transfer)

$$Sc^{3+}(DMSO)_n \rightarrow Sc^{2+}(DMSO)_{n-1} + DMSO^+$$

(b) Loss of protonated DMSO (proton transfer)

$$Sc^{3+}(DMSO)_n \rightarrow Sc^{2+}(CH_3CH_2SO)(DMSO)_{n-2} + H^+DMSO$$

(c) Loss of a methyl radical (CH_3)

$$Sc^{3+}(DMSO)_n \rightarrow Sc^{3+}(CH_3SO)(DMSO)_{n-1} + CH_3$$

(d) Loss of methane (CH_4)

$$Sc^{3+}(DMSO)_n \rightarrow Sc^{3+}(CH_2SO)(DMSO)_{n-1} + CH_4$$

(e) Loss of a methyl radical cation (CH_3^+)

$$Sc^{3+}(DMSO)_n \rightarrow Sc^{2+}(CH_3SO)(DMSO)_{n-1} + CH_3^+$$

(f) Loss of a methane cation (CH_4^+)

$$Sc^{3+}(DMSO)_n \rightarrow Sc^{2+}(CH_2SO)(DMSO)_{n-1} + CH_4^+$$

(g) Double methyl radical loss ($2CH_3$)

$$Sc^{3+}(DMSO)_n \rightarrow Sc^{3+}(CH_3SO)_2(DMSO)_{n-2} + 2CH_3$$

(h) Double methane loss ($2CH_4$)

$$Sc^{3+}(DMSO)_n \rightarrow Sc^{3+}(CH_2SO)_2(DMSO)_{n-2} + 2CH_4$$

(i) Sequential loss of CH_3 and CH_4

$$Sc^{3+}(DMSO)_n \rightarrow Sc^{3+}(CH_2SO)(CH_3SO)(DMSO)_{n-2} + CH_3 + CH_4$$

Processes c, d, and g−i correspond to the loss of neutral fragments, while charge separation is involved in processes a, b, e, and f. In the experimental work of Shvartsburg,[25] products with the loss of CH_3, CH_4, CH_3^+, $2CH_3$, $2CH_4$, and $CH_3 + CH_4$ were all observed for selected species, while electron- and proton-transfer processes were not observed. The loss of a methane cation (CH_4^+) was not observed either, but it may be interesting to consider this process for comparison with the loss of CH_3^+.

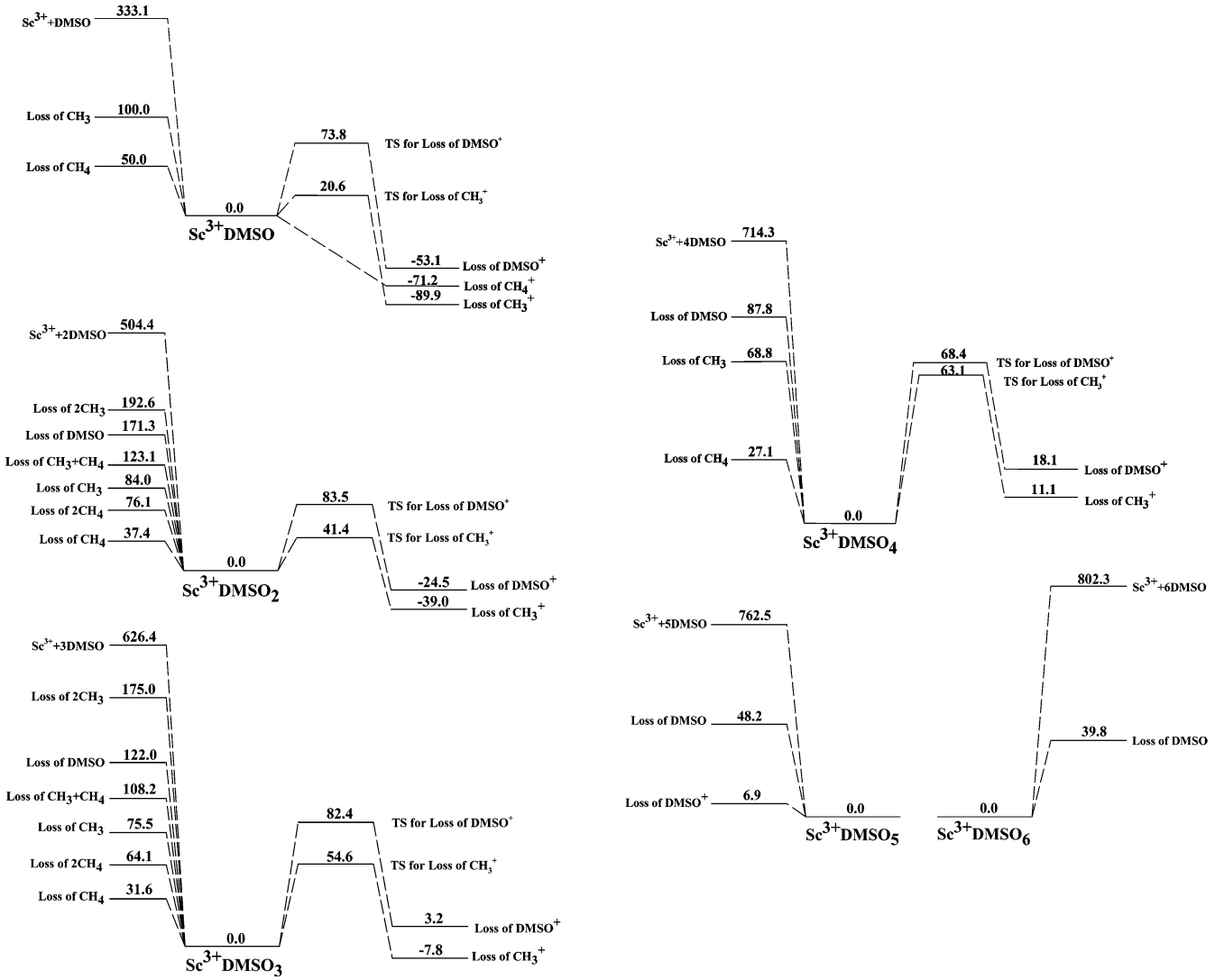

Figure 5. Dissociation energies (in kcal/mol) for various dissociation channels of $Sc^{3+}DMSO_n$ and energy barriers as determined by the corresponding transition states (TS), calculated at the B3LYP/6-311+G(d, p) level.

First of all, we point out that the geometry optimization for the dissociated product of the proton-transfer process b, $Sc^{2+}(CH_3CH_2SO)(DMSO)_{n-2}$, always led to two separated fragments $Sc^{+}O(DMSO)_{n-2} + CH_3SCH_2^{+}$ ($n = 2-5$). This finding may explain why the proton-transfer induced products were not experimentally observed. Therefore, this process is not considered in the following discussion. It is worth mentioning that both $Sc^{+}O(DMSO)_{n-2}$ ($n = 2-4$) and $CH_3SCH_2^{+}$ fragments were experimentally observed,[25] although their origins are unclear. In this context, it should be noted that the emergence of $CH_3SCH_2^{+}$ might also be related to a rupture of the S=O bond in DMSO combined with a concomitant proton transfer from a methyl group to oxygen, as described in ref 25.

The equilibrium structures for products of all other dissociation processes and the transition states for the charge-separating processes a and e of $Sc^{3+}(DMSO)_n$ up to $n = 3$ were determined and are presented in Figures 1−3. Geometric parameters and natural charges are available in the Supporting Information.

For $Sc^{3+}(DMSO)_4$, all but the two-step processes (g−i) were studied since we found from the calculation of $Sc^{3+}(DMSO)_2$ and $Sc^{3+}(DMSO)_3$ that the dissociation energies of the two-step processes can be estimated by the sum of the dissociation energies of the relevant one-step processes (see Section III.B. below). For $Sc^{3+}(DMSO)_5$ and $Sc^{3+}(DMSO)_6$, only the electron-transfer process was considered. For the sake of brevity, we do not present or describe in detail the structures of the dissociation products of these larger complexes, but their energetics will be discussed in the following subsection.

The loss of $DMSO^{+}$ from $Sc^{3+}(DMSO)_n$ yields ligated dications of diminished size, $Sc^{2+}(DMSO)_{n-1}$. The structures of $Sc^{2+}(DMSO)_n$ up to $n = 3$ are presented in Figures 1−3. From these figures, one finds that the $Sc^{2+}(DMSO)_n$ species take similar structures to the corresponding $Sc^{3+}(DMSO)_n$ units, and the bond angles and S−C bond lengths of the two species are quite close. The Sc−O and O−S bond lengths, however, are elongated and shortened, respectively.

The loss of CH_3 or CH_4 leads mainly to the elongation of the Sc−O and the contraction of the O−S and S−C bond lengths of the cleaved DMSO, while the remaining part is only slightly modified. For the loss of CH_4, we have considered both the cleavage of all atoms from the same DMSO and the cleavage of one H atom from another DMSO and found that the former process is energetically more favorable than the latter.

III.B. Energetics. The dissociation energies for various processes and the energy barriers formed by the transition states for the charge-separating processes a and e of $Sc^{3+}(DMSO)_n$ are displayed in Figure 5. In addition, the dissociation energies in the following two processes are calculated:

(j) Dissociation into free metal and ligands

$$Sc^{3+}(DMSO)_n \rightarrow Sc^{3+} + n\text{DMSO}$$

(k) Loss of neutral DMSO

$$Sc^{3+}(DMSO)_n \rightarrow Sc^{3+}(DMSO)_{n-1} + \text{DMSO}$$

Process j involves the binding energy related to the bond between Sc and its ligands, while process k is the only dissociation channel in bulk solution. For all processes a−k, the dissociation energy is defined as the difference between the energy of the initial complex (set to zero in Figure 5) and the total energy of the disintegration products.

From Figure 5, we arrive at the following conclusions:

III.B.1. Binding of $Sc^{3+}(DMSO)_n$. The binding energy of $Sc^{3+}(DMSO)_n$ is large and is higher than those reported for many dicationic complexes $M^{2+}L$ (L = H_2O, NH_3, acetone, formaldehyde, and DMSO),[26−28,32] indicating that the interaction between Sc^{3+} and the DMSO ligands is strong.

III.B.2. Dissociation of $Sc^{3+}(DMSO)_n$ without Charge Separation. All dissociation processes of $Sc^{3+}(DMSO)_n$ without charge separation (c, d, g−k) are endothermic (positive dissociation energy). Thus, the $Sc^{3+}(DMSO)_n$ species of all sizes are thermodynamically stable with respect to these dissociation channels.

For all complex sizes, the order in the dissociation energies (E_d) is E_d(loss of CH_4) < E_d(loss of $2CH_4$) < E_d(loss of CH_3) < E_d(loss of $CH_3 + CH_4$) < E_d(loss of DMSO) < E_d(loss of $2CH_3$). Therefore, for the one-step processes, the cleavage of CH_4 is energetically more favorable than the loss of CH_3, and both are more favorable than the loss of neutral DMSO. As for the two-step processes, it is interesting to note that their dissociation energies are very close to the sum of the dissociation energies of the relevant one-step processes.

Since the dissociation energy for the loss of CH_4 is only half or even less than half the value for the loss of CH_3, the loss of $2CH_4$ is more favorable than the loss of CH_3. This finding may lead to the expectation to detect more products related to the loss of CH_4 than of CH_3. Experimentally,[25] however, products originating from the loss of CH_3 and CH_4 were observed for both $Sc^{3+}(DMSO)_3$ and $Sc^{3+}(DMSO)_4$, and products from the loss of $CH_3 + CH_4$ and $2CH_3$ were observed for $Sc^{3+}(DMSO)_3$. It may appear puzzling that the loss of $2CH_4$ is not observed at any complex size, although the dissociation energy for this process is lower than the loss of CH_3. One possible reason is that the loss of CH_3 is a one-step dissociation reaction while the loss of CH_4 can be considered to be a reaction which would involve two substeps, namely, first the formation and then the loss of CH_4, since the CH_3 unit already exists in DMSO but CH_4 does not. Therefore, a double energy barrier on a complicated potential energy surface would have to be overcome for the loss of CH_4, and the loss of $2CH_4$ would involve four substeps with two double-barriers and thus a process of much greater complexity than the loss of $2CH_3$. A detailed exploration of this mechanism will be very interesting and a topic for further research. A similar problem was explored by Beyer et al.[8] on the mechanism of the proton-transfer reaction $M^{2+}(H_2O)_2 \rightarrow MOH^+ + H_3O^+$.

III.B.3. Dissociation of $Sc^{3+}(DMSO)_n$ with Charge Separation. The dissociation processes of the $Sc^{3+}(DMSO)_n$ species with charge separation (a, e) are exothermic (negative dissociation energy) for $n = 1-3$ and endothermic for $n \geq 4$. Therefore, the $Sc^{3+}DMSO_n$ complexes with $n = 1-3$ are thermodynamically unstable with respect to these two processes and would dissociate spontaneously by Coulombic repulsion unless a sufficiently high energy barrier exists to resist the process. For the $Sc^{3+}DMSO_n$ species with $n \geq 4$, these two dissociation processes are energetically unfavorable, but the dissociation energies are lower than those for any processes without charge separation (c, d, g−k). Therefore, the small $Sc^{3+}DMSO_n$ complexes indeed have a strong intrinsic tendency for charge separation.

For comparison, we have calculated the dissociation energies for the electron-transfer process of doubly charged $Sc^{2+}(DMSO)_n$ complexes with $n = 1-3$ and found that this process is endothermic for all sizes. The calculated dissociation energies for this process with $n = 1-3$ are 42.4, 64.8, and 79.3 kcal/mol, respectively. Therefore, the doubly charged $Sc^{2+}(DMSO)_n$ species of all sizes are thermodynamically stable with respect to electron transfer.

We have determined the transition states for $Sc^{3+}DMSO_n$ in processes a and e up to $n = 4$ (see Figures 1−3, 5). Frequency analysis confirmed that these transition states have only one imaginary frequency which corresponds to the stretching mode of the cleaved bond between the separated $DMSO^+$ or CH_3^+ fragment and the remaining product. The energy difference between the transition state and the equilibrium structure $Sc^{3+}DMSO_n$ then defines an energy barrier of the corresponding dissociation process, which is calculated to be 73.8, 83.5, 82.4, and 68.4 kcal/mol for process a and 20.6, 41.4, 54.6, and 63.1 kcal/mol for process e with $n = 1-4$. Because of the existence of these sufficiently high energy barriers, the $Sc^{3+}(DMSO)_n$ species with $n = 1-3$ are kinetically metastable against the charge-separating processes a and e. In addition, since both the dissociation energy and the energy barrier for process a are higher than the corresponding data for process e for all sizes, the cleavage of CH_3^+ is more favorable than the electron-transfer process. This agrees with the fact that the cleavage of CH_3^+ was observed (for $n = 3$) but the dissociative electron transfer was not in the experiment of Shvartsburg.[25]

We do not attempt a complete description of the dissociation through loss of CH_4^+. For Sc^{3+}DMSO, however, we investigated this process and found the corresponding dissociation energy to be comparable to that for the loss of CH_3^+. Whether this dissociation process can take place depends on the respective energy barrier. Determination of the transition state for this process, however, would be challenging because of the complicated double energy barrier as discussed above. The absence of such products in Shvartsburg's experiment[25] implies a high energy barrier for this disintegration pathway.

III.B.4. Two Possible Channels for the Product $Sc^{2+}(CH_3SO)(DMSO)_n$. In the experiment of Shvartsburg,[25] the product $Sc^{2+}(CH_3SO)(DMSO)_n$ was observed with $n = 1$ and 2, and two possible dissociation channels were proposed to produce it. The first one is by the loss of CH_3^+ from $Sc^{3+}(DMSO)_{n+1}$ (process e) and the second one is by the loss of $DMSO^+$ from $Sc^{3+}(CH_3SO)(DMSO)_{n+1}$

(l) $$Sc^{3+}(CH_3SO)(DMSO)_{n+1} \rightarrow Sc^{2+}(CH_3SO)(DMSO)_n + \text{DMSO}^+$$

Since the observed CH_3^+ yield was minute, process l was suggested to be the major pathway.

To examine which mechanism is more favorable, we have calculated the dissociation energies for these two processes. Because $Sc^{3+}CH_3SO(DMSO)_{n+1}$ is itself a product that needs to be derived from the available parent ion, it is not appropriate to directly compare the dissociation energy for process e with that for process l. Rather, the total dissociation energy from

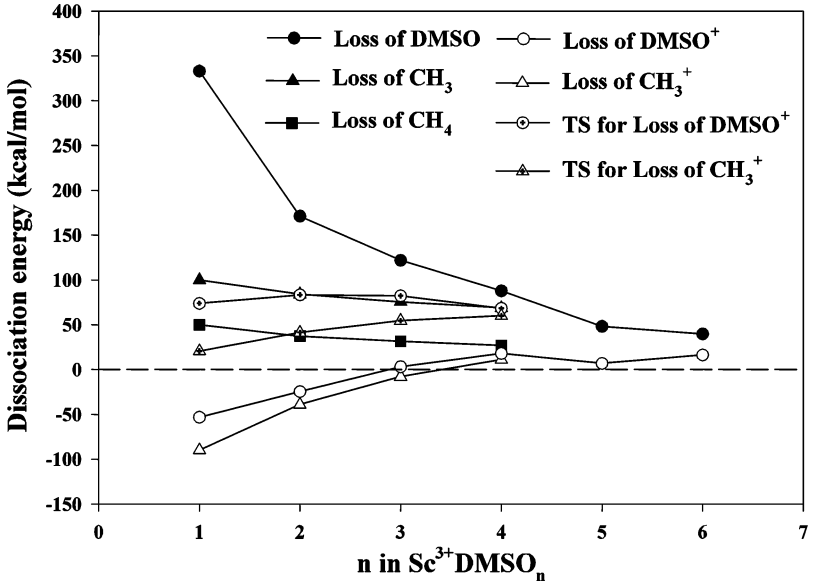

Figure 6. Size dependence of the dissociation energies and energy barriers for various dissociation channels of $ScDMSO_n$, calculated at the B3LYP/6-311+G(d, p) level.

$Sc^{3+}(DMSO)_{n+2}$ reactant to $Sc^{2+}CH_3SO(DMSO)_n$ product should be compared along two different two-step pathways: (α) loss of CH_3^+ followed by DMSO evaporation

$$(\alpha\text{-}1)\ Sc^{3+}(DMSO)_{n+2} \rightarrow Sc^{2+}(CH_3SO)(DMSO)_{n+1} + CH_3^+$$

$$(\alpha\text{-}2)\ Sc^{2+}(CH_3SO)(DMSO)_{n+1} \rightarrow Sc^{2+}(CH_3SO)(DMSO)_n + DMSO$$

and (β) cleavage of CH_3 followed by $DMSO^+$ loss

$$(\beta\text{-}1)\ Sc^{3+}(DMSO)_{n+2} \rightarrow Sc^{3+}(CH_3SO)(DMSO)_{n+1} + CH_3$$

$$(\beta\text{-}2)\ Sc^{3+}(CH_3SO)(DMSO)_{n+1} \rightarrow Sc^{2+}(CH_3SO)(DMSO)_n + DMSO^+$$

We have calculated the total dissociation energies for these two processes with $n = 0-2$, which is the sum of the dissociation energies for the two substeps of each process. The calculated values are 80.0−83.1 kcal/mol for process α and 52.4−55.5 kcal/mol for process β. Therefore, our calculated result supports the mechanism suggested in ref 25.

III.B.5. The Minimum Size. From the above discussion, we can conclude that the minimum number of DMSO ligands required to stabilize the Sc^{3+} trication against electron transfer is $n_{min} = 1$. However, a larger value of $n_{min} = 3$ was reported in the experimental work of Shvartsburg.[25]

To understand this disagreement, we note that a similar discrepancy occurred recently concerning the stability of $Cu^{2+}(H_2O)_n$ that led to a lively debate between theory and experiment. Earlier experimental attempts using the ESI technique[21,39,40] failed to produce any $Cu^{2+}(H_2O)_n$ complexes, and the authors concluded that at least 15 H_2O molecules are needed to stabilize Cu^{2+}. This minimum number was later reduced to 3 by Stace et al.[41,42] using the "pick-up" technique. Recently, a calculation by El-Nahas et al.[26,43] using the B3LYP method predicted that Cu^{2+} ligated with a single H_2O molecule can be kinetically metastable against the dissociative electron transfer with an energy barrier of 6.4 kcal/mol and suggested that it could be detectable at refined experimental conditions. This prediction was soon confirmed by Shvartsburg et al.[9] and Stone et al.[29] using the ESI, as well as by Schröder et al.[30] using the charge-stripping technique, respectively. Since a similar theoretical method is used in our calculation, it appears conceivable that the $Sc^{3+}(DMSO)_n$ complexes with $n = 1$, 2 could be detected in future refined charge-stripping or electrospray ionization measurements, selecting proper pathways to reach mono- and diligated $Sc^{3+}(DMSO)_n$ units.

III.B.6. The Critical Size. Finally, we discuss the critical size above which the evaporation of neutral ligand will become more favorable than dissociative electron or proton transfer.

Figure 6 shows the size dependence of the dissociation energies and energy barriers for various dissociation channels of $Sc^{3+}(DMSO)_n$. The dissociation energies for the processes without charge separation (c, d, k) all decrease with increasing complex sizes and that for the loss of neutral DMSO drops much faster than the other processes. In contrast, the dissociation energies for the processes with charge separation (a, e) both increase with increasing complex sizes. The energy-barrier curves of these processes follow a similar rising trend. As a result, the evaporation of neutral DMSO ligand becomes more favorable while the electron-transfer process becomes less preferred with increasing size. It can be expected that these two curves will cross at a critical size (n_{crit}) above which the evaporation of neutral ligand will become more favorable than the electron-transfer process. In the absence of any energy barrier, this number is estimated to be $n_{crit} = 7-8$. However, for any process to actually take place, the energy barrier must be overcome. This hinders the electron-transfer process and reduces the critical size to $n_{crit} = 5-6$.

We want to point out that from our data referring to both the dissociation energy and the activation energy barrier associated with the loss of CH_3^+, as displayed in Figure 6, the species $Sc^{2+}CH_3SO(DMSO)_n$ with $n = 3$ can be expected to be experimentally observable while ref 25 only reports products of CH_3^+ loss up to $n = 2$. Further, it is noteworthy that, from Table 1 of ref 25, the loss of CH_3 has been found for complexes up to $Sc^{3+}(DMSO)_4$. This is compatible with the trend of the dissociation energy curve in Figure 6 for the loss of CH_3, which might be extrapolated to show a crossover with the respective curve for DMSO in the region $n = 4$ to 5.

IV. Summary

This contribution describes a comprehensive theoretical study on $Sc^{3+}(DMSO)_n$ complexes up to $n = 6$ at the B3LYP/6-311+G(d, p) level. We performed this work in order to understand the structures and stabilities of these complexes with respect to various dissociation processes. The main conclusions can be summarized as follows:

(1) The equilibrium structures of $Sc^{3+}(DMSO)_n$ are determined and the nature of the stationary points is characterized by frequency analysis. The Sc^{3+} ion is attached to the oxygen atoms of the DMSO ligands. The most stable structures of $Sc^{3+}(DMSO)_n$ correspond to highly symmetric and quasi-spherical ones, namely, a bent structure for $Sc^{3+}(DMSO)_2$, an equilateral triangle for $Sc^{3+}(DMSO)_3$, a regular tetrahedron for $Sc^{3+}(DMSO)_4$, a trigonal bipyramid for $Sc^{3+}(DMSO)_5$, and a regular octahedron for $Sc^{3+}(DMSO)_6$.

(2) The stabilities of $Sc^{3+}(DMSO)_n$ complexes with respect to a variety of dissociation processes are examined. These processes include the evaporation of neutral DMSO, the dissociative electron and proton transfer, the cleavage of a methyl radical or a methyl cation (CH_3 and CH_3^+), the cleavage of neutral methane (CH_4), and a combined cleavage of a methyl radical and methane ($2CH_3$, $2CH_4$, and $CH_3 + CH_4$). In addition, the cleavage of a methane cation (CH_4^+) is studied for the monoligated complex in order to compare with the cleavage of CH_3^+.

The equilibrium structures of these dissociated products are determined, and the dissociation energies are calculated. For the dissociation processes with charge separation (dissociative electron transfer and cleavage of CH_3^+), the transition states and energy barriers up to $n = 4$ are also determined.

All dissociation processes without charge separation are endothermic for all sizes. Therefore, the $Sc^{3+}(DMSO)_n$ complexes ($n = 1-6$) are thermodynamically stable with respect to these dissociation channels.

The dissociation processes of $Sc^{3+}(DMSO)_n$ complexes with charge separation (dissociative electron transfer and cleavage of CH_3^+) are exothermic for $n = 1-3$ and endothermic for $n \geq 4$. Therefore, the larger $Sc^{3+}(DMSO)_n$ species ($n \geq 4$) are thermodynamically stable, while the smaller $Sc^{3+}(DMSO)_n$ species ($n = 1-3$) are thermodynamically unstable with respect to these dissociation channels. However, these smaller species are found to be kinetically metastable with respect to the considered charge-separation channels, due to the existence of sufficiently high energy barriers.

(3) The minimum size at which the $Sc^{3+}(DMSO)_n$ complex is stable against a spontaneous electron or proton transfer is $n_{min} = 1$ from our calculation. This number is smaller than the value of 3 determined in a recent experiment. A similar discrepancy appeared also for $Cu^{2+}(H_2O)_n$ between theory and experiment, but the theoretical prediction was confirmed by the most recent observations at refined experimental conditions.[29,30] Therefore, we suggest further experiments on $Sc^{3+}(DMSO)_n$ to examine our prediction.

(4) The critical size, above which the evaporation of neutral ligands becomes more favorable than the dissociative electron or proton transfer, is estimated to be $n_{crit} = 5-6$ by examining the size dependence of the dissociation energies for the neutral ligand loss and electron-transfer processes.

In the future effort, we plan to extend this work to various related, yet unexplored, problems, such as the transition state and energy barrier for the loss of CH_4^+, and also to analyze complexes of metals and ligands other than Sc and DMSO along the lines followed in this contribution.

Acknowledgment. This work is supported by the National Science Foundation through Grants HRD-9805465, NSF-0132618, and DMR-0304036, by the National Institutes of Health through Grant S06-GM008047, and by the Army High Performance Computing Research Center under the auspices of the Department of the Army, Army Research Laboratory, under Cooperative Agreement No. DAAD 19-01-2-0014. The authors thank Dr. Alexandre A. Shvartsburg for valuable suggestions. We are grateful to Dr. Jianhua Wu for his help with the preparation of the manuscript.

Note Added after ASAP Posting. The structure CH_3^+ was removed from the Abstract and the term methyl radical cation was changed to methyl cation in the ninth paragraph of the Introduction and the third paragraph of the Summary in the version posted ASAP June 2, 2004; the corrected version was posted June 4, 2004.

Supporting Information Available: Tables 1S−4S present the geometrical data and natural charges for $Sc^{3+}(DMSO)_n$ ($n = 1-6$), various dissociated products, and related transition states. This material is available free of charge via the Internet at http://pubs.acs.org.

References and Notes

(1) Marcus, Y. *Ion Solvation*; John Wiley: New York, 1985.
(2) Castleman, A. W.; Bowen, K. H. *J. Phys. Chem.* **1996**, *100*, 12911.
(3) Lisy, J. M. *Int. Rev. Phys. Chem.* **1997**, *16*, 267.
(4) Karlin, K. D. *Science* **1993**, *261*, 701.
(5) Siegbahn P. E. M.; Bloomberg, M. R. A. *Chem. Rev.* **2000**, *100*, 421.
(6) Wright, R. R.; Walker, N. R.; Firth, S.; Stace, A. J. *J. Phys. Chem. A* **2001**, *105*, *54*.
(7) Spears K. J.; Fehsenfeld, F. C. *J. Chem. Phys.* **1972**, *56*, 5698.
(8) Beyer, M.; Williams, E. R.; Bondybey, V. E. *J. Am. Chem. Soc.* **1999**, *121*, 1565.
(9) Shvartsburg, A. A.; Siu, K. W. M. *J. Am. Chem. Soc.* **2001**, *123*, 10071.
(10) Jayaweera, P.; Blades, A. T.; Ikonomou, M. G.; Kebarle, P. *J. Am. Chem. Soc.* **1990**, *112*, 2452.
(11) Dobson, M. P.; Stace, A. J. *Chem. Commun.* **1996**, 1533.
(12) Schröder, D.; Schwarz, H. *J. Phys. Chem. A* **1999**, *103*, 7385.
(13) Anderson, U. N.; Bojesen, G. *Int. J. Mass Spectrom. Ion Processes* **1996**, *153*, 1.
(14) Kohler, M.; Leary, J. A. *Int. J. Mass Spectrom. Ion Processes* **1997**, *162*, 17.
(15) Walker, N. R.; Wright, R. R.; Stace, A. J. *J. Am. Chem. Soc.* **1999**, *121*, 4837.
(16) Peschke, M.; Blades, A. T.; Kebarle, P. *Int. J. Mass Spectrom.* **1999**, *185/186/187*, 685.
(17) Shvartsburg, A. A.; Wilkes, J. G.; Lay, J. O.; Siu, K. W. M. *Chem. Phys. Lett.* **2001**, *350*, 216.
(18) Shvartsburg, A. A.; Wilkes, J. G. *J. Phys. Chem. A* **2002**, *106*, 4543.
(19) Shvartsburg, A. A.; Wilkes, J. G. *Int. J. Mass Spectrom.* **2003**, *225*, 155.
(20) Shvartsburg, A. A. *J. Am. Chem. Soc.* **2002**, *124*, 7910.
(21) Blades, A. T.; Jayaweera, P.; Ikonomou, M. G.; Kebarle, P. *Int. J. Mass Spectrom. Ion Processes* **1990**, *101*, 325.
(22) Cheng, Z. L.; Siu, K. W. M.; Guevremont, R.; Berman, S. S. *Org. Mass Spectrom.* **1992**, *27*, 1370.
(23) Walker, N. R.; Wright, R. R.; Stace, A. J.; Woodward, C. A. *Int. J. Mass Spectrom.* **1999**, *188*, 113.
(24) Shvartsburg, A. A. *Chem. Phys. Lett.* **2002**, *360*, 479.
(25) Shvartsburg, A. A. *J. Am. Chem. Soc.* **2002**, *124*, 12343.
(26) El-Nahas, A. M.; Tajima, N.; Hirao, K. *Chem. Phys. Lett.* **2000**, *318*, 333.
(27) El-Nahas, A. M. *Chem. Phys. Lett.* **2001**, *345*, 325.
(28) El-Nahas, A. M. *Chem. Phys. Lett.* **2002**, *365*, 251.
(29) Stone J. A.; Vukomanovic, D. *Chem. Phys. Lett.* **2001**, *346*, 419.
(30) Schröder, D.; Schwarz, H.; Wu, J.; Wesdemiotis, C. *Chem. Phys. Lett.* **2001**, *343*, 258.

(31) Bérces, A.; Nukada, T.; Margl, P.; Ziegler, T. *J. Phys. Chem. A* **1999**, *103*, 9693.
(32) El-Nahas, A. M. *Chem. Phys. Lett.* **2001**, *348*, 483.
(33) Stone, J. A.; Su, T.; Vukomanovic, D. *Int. J. Mass Spectrom.* **2002**, *216*, 219.
(34) Frisch, M. J.; Trucks, G. W.; Schlegel, H. B.; Scuseria, G. E.; Robb, M. A.; Cheeseman, J. R.; Zakrzewski, V. G.; Montgomery, J. A., Jr.; Stratmann, R. E.; Burant, J. C.; Dapprich, S.; Millam, J. M.; Daniels, A. D.; Kudin, K. N.; Strain, M. C.; Farkas, O.; Tomasi, J.; Barone, V.; Cossi, M.; Cammi, R.; Mennucci, B.; Pomelli, C.; Adamo, C.; Clifford, S.; Ochterski, J.; Petersson, G. A.; Ayala, P. Y.; Cui, Q.; Morokuma, K.; Malick, D. K.; Rabuck, A. D.; Raghavachari, K.; Foresman, J. B.; Cioslowski, J.; Ortiz, J. V.; Stefanov, B. B.; Liu, G.; Liashenko, A.; Piskorz, P.; Komaromi, I.; Gomperts, R.; Martin, R. L.; Fox, D. J.; Keith, T.; Al-Laham, M. A.; Peng, C. Y.; Nanayakkara, A.; Gonzalez, C.; Challacombe, M.; Gill, P. M. W.; Johnson, B. G.; Chen, W.; Wong, M. W.; Andres, J. L.; Head-Gordon, M.; Replogle, E. S.; Pople, J. A. *Gaussian 98*, revision A.9; Gaussian, Inc.: Pittsburgh, PA, 1998.
(35) Becke, A. D. *J. Chem. Phys.* **1993**, *98*, 5648.
(36) Lee, C.; Yang, W.; Parr, R. G. *Phys. Rev. B* **1988**, *37*, 785.
(37) Boys, S. F.; Bernardi, F. *Mol. Phys.* **1976**, *19*, 325.
(38) Carpenter, J. E.; Weinhold, F. *J. Mol. Struct. (THEOCHEM)* **1988**, *169*, 41.
(39) Blades, A. T.; Jayaweera, P.; Ikonomou, M. G.; Kebarle, P. *Int. J. Mass Spectrom. Ion Processes* **1990**, *102*, 251.
(40) Blades, A. T.; Jayaweera, P.; Ikonomou, M. G.; Kebarle, P. *J. Chem. Phys.* **1990**, *92*, 5900.
(41) Stace, A. J.; Walker, N. R.; Firth, S. *J. Am. Chem. Soc.* **1997**, *119*, 10239.
(42) Stace, A. J.; Walker, N. R.; Wright, R. R.; Firth, S. *Chem. Phys. Lett.* **2000**, *329*, 173.
(43) El-Nahas, A. M. *Chem. Phys. Lett.* **2000**, *329*, 176.